Atmospheric CO2 modeling at the regional scale: an intercomparison of 5 meso-scale atmospheric models

C. Sarrat, J. Noilhan, A. J. Dolman, C. Gerbig, R. Ahmadov, L. F. Tolk, A. G. C. A. Meesters, R. W. A. Hutjes, H. W. ter Maat, G. Pérez-Landa, et al.

Biogeosciences, 4, 1115–1126, 2007
www.biogeosciences.net/4/1115/2007/

Biogeosciences

Atmospheric CO_2 modeling at the regional scale: an intercomparison of 5 meso-scale atmospheric models

C. Sarrat[1], J. Noilhan[1], A. J. Dolman[2], C. Gerbig[3], R. Ahmadov[3], L. F. Tolk[2], A. G. C. A. Meesters[2], R. W. A. Hutjes[4], H. W. Ter Maat[4], G. Pérez-Landa[5], and S. Donier[5]

[1]CNRM-GAME Météo France, 42 avenue Coriolis, 31057 Toulouse cedex France
[2]Vrije Universiteit, De Boelelaan 1085,1081 HV Amsterdam, The Netherlands
[3]Max Planck Institute for Biogeochemistry,Hans-Knoell-Str.10, 07745 Jena, Germany
[4]ALTERRA, Droevendaalsesteeg 3, 6708 PB Wageningen,The Netherlands
[5]CEAM,Parque Tecnológico C/Charles R. Darwin, 14, 46980-Paterna-Valencia, Spain

Received: 21 May 2007 – Published in Biogeosciences Discuss.: 25 June 2007
Revised: 18 October 2007 – Accepted: 2 November 2007 – Published: 17 December 2007

Abstract. Atmospheric CO_2 modeling in interaction with the surface fluxes, at the regional scale is developed within the frame of the European project CarboEurope-IP and its Regional Experiment component. In this context, five meso-scale meteorological models at 2 km resolution participate in an intercomparison exercise. Using a common experimental protocol that imposes a large number of rules, two days of the CarboEurope Regional Experiment Strategy (CERES) campaign are simulated. A systematic evaluation of the models is done in confrontation with the observations, using statistical tools and direct comparisons. Thus, temperature and relative humidity at 2 m, wind direction, surface energy and CO_2 fluxes, vertical profiles of potential temperature as well as in-situ CO_2 concentrations comparisons between observations and simulations are examined. These comparisons reveal a cold bias in the simulated temperature at 2 m, the latent heat flux is often underestimated. Nevertheless, the CO_2 concentrations heterogeneities are well captured by most of the models.
This intercomparison exercise shows also the models ability to represent the meteorology and carbon cycling at the synoptic and regional scale in the boundary layer, but also points out some of the major shortcomings of the models.

1 Introduction

Atmospheric measurements of CO_2, mainly from remote islands, have been a major source of information about the global scale spatial distribution and temporal changes in CO_2 exchange fluxes between ocean-atmosphere as well as land-atmosphere (Tans et al., 1990; Bousquet et al., 1998; Rödenbeck et al., 2003).

However, to retrieve more detailed information of the controlling processes, measurements in the planetary boundary layer over land, have to be made. These measurements show that the spatio-temporal variability, such as derived from aircraft data over continents is very large and exhibits small correlation length scales (e.g. Gerbig et al., 2003). Thus, for any modelling interpretation, high resolution mesoscale models need to be used to resolve this variability. Moreover, in order to retrieve CO_2 sources and sinks at the regional scale, we need to estimate how the meso-scale models are able to reproduce the CO_2 transport and surface fluxes. The evaluation of the meteorological models is a first step towards inverse regional modeling and sources and sinks retrieval (Lauvaux et al., 2007).

Recent studies have shown the ability of meso-scale models to simulate correctly the surface energy and CO_2 fluxes as well as atmospheric CO_2 concentrations (Pérez-Landa et al., 2007; Sarrat et al., 2007; Ahmadov et al., 2007).

This study describes a first intercomparison of CO_2 modeling at the meso-scales, typically over an area of 300 km by 300 km, at 2 km resolution, allowing the evaluation of the models at the regional scale. The regional experiment of the European project CarboEurope-IP took place in May and June 2005. The CarboEurope Regional Experiment Strategy (CERES) campaign aimed at measuring and budgeting the atmospheric CO_2. The project is described in detail by Dolman et al. (2006). A dense experimental network represented in Fig. 1, has been deployed in the South-West of France, in Les Landes forest, including 10 surface fluxes stations over several ecosystems (vineyard, maize, wheat, rapeseed, pine forest, fallow). The main sites used in this study

Correspondence to: C. Sarrat
(claire.sarrat@cnrm.meteo.fr)

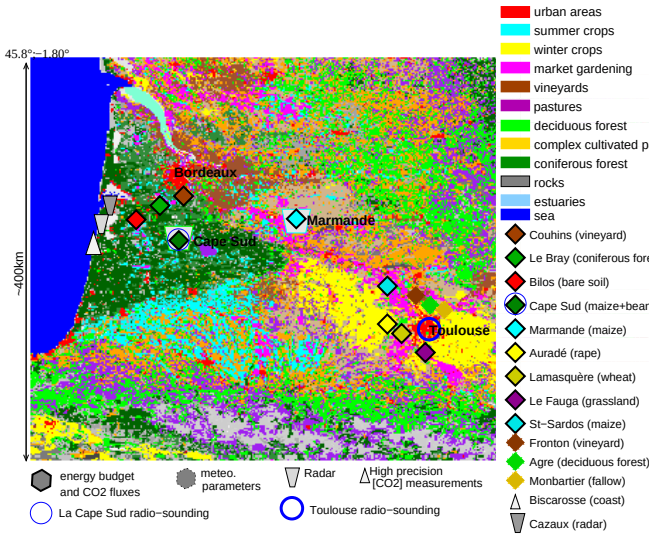

Fig. 1. Map of the experimental network that corresponds approximatively to the domain of simulation at 2 km.

are briefly described in Table 1. In the pine forest, the evolution of the Atmospheric Boundary Layer (ABL) was monitored with 3-hourly radio-soundings and a UHF radar. CO_2 concentrations were measured continuously near the Atlantic coast line on the West and above the agricultural area on the East. Four research aircrafts were deployed over the region in order to measure the vertical and horizontal distribution of CO_2 during Intensive Observing Periods (IOPs). Using the full suite of data obtained in CERES provides a stringent test of the models, as we can compare both surface fluxes, boundary layer development and the transport of CO_2 through the domain.

The evaluation of the model behavior is based on simulations of two cases during the different CERES intensive observational periods (IOP2 and IOP4, Dolman et al., 2006). Two contrasting days of the campaign are simulated with the meso-scale models following a precise protocol: the 27 May and the 6 June 2005 (hereafter respectively 27 May and 6 June).

27 May is the fourth day of the IOP 2 and is very well documented with 7 aircraft flights. This is a very warm day in an anticyclonic synoptic situation, with temperature reaching 32°C in les Landes. The wind is weak, from South-East in the morning and turning to North-West in the afternoon near the coast because of the sea breeze development.

The second day for simulation is 6 June. It corresponds to the IOP4, the Lagrangian experiment. This has also been well documented with aircraft observations. The day is colder than the 27 May and the North-West wind is homogeneous and regular over the entire domain during all day.

Table 1. Description of the sites where surface observations are made.

Name	Acronym	Type of site	Location
La Bray	LEBR	Pine forest	East – forest
La Cape Sud	LACS	Summer crops (maize and beans)	East – forest
Auradé	AURA	Winter crop	East of the domain
Marmande	MARM	Summer crops	Middle of the domain
Toulouse	TOUL	Suburban place	East of the domain

2 Models set-up

Five models are participating in this intercomparison.

The experimental conditions have been briefly described above. All the models are set according the same configuration:

- All models use nested configuration with the resolution set at 2 km for the smallest domain (Fig. 1).
- The meteorological variables and surface parameters such as soil moisture are initialized by the ECMWF analysis (the soil water content from ECMWF was compared with the observations taken over 30 cm in Table 2).
- Meteorological lateral boundaries conditions are also provided by the ECMWF analysis fields.
- The ECOCLIMAP land cover database (Champeaux et al., 2005) is set as the standard for land cover distribution for all models.
- Sand and clay distributions are taken from the FAO classification.
- Anthropogenic emissions of CO_2 are issued from the Stuttgart University inventory at 10 km hourly resolution.
- Orography and vertical resolution are chosen individually for each model, but are generally taken from similar databases and show no major differences between models.

The models participating in the intercomparison are: the Weather Research and Forecasting model (WRF), Meso-NH and 3 different versions of Regional Atmospheric Modeling System (RAMS). The models and their set-up are briefly described in the following sections and summurized in Table 3.

2.1 The WRF model

The Max-Planck Institute (MPI) for Biogeochemistry ran the Weather Research and Forecasting (WRF) model (Skamarock et al., 2005) for meteorology and CO_2 transport. Biospheric CO_2 fluxes are simulated with a diagnostic

model, the Vegetation Photosynthesis and Respiration Model (VPRM, Pathmathevan et al., 2006), using temperature and radiation from WRF, EVI and LSWI satellite indices calculated from MODIS (Moderate Resolution Imaging Spectroradiometer) reflectances. A detailed description of the WRF-VPRM modeling system is given in Ahmadov et al. (2007). Hereafter, the WRF results from MPI are designated by WRF-MPI.

The main characteristics of the model set-up are :

- The model was run on two grids with 2 and 6 km resolution, on two-way nesting mode.
- Land cover from the USGS land-use (24 classes) and NCEP vegetation fraction data.
- CO_2 concentrations initialized with a homogeneous vertical profile and/or the LMDZ simulations. CO_2 fields from LDMZ were also used for CO_2 boundary conditions.
- No CO_2 sea fluxes prescribed.

2.2 The RAMS version from the Vrije Universiteit team

The Amsterdam Vrije Universiteit used the regional atmospheric model BRAMS-3.2 (Brazilian version of RAMS, Freitas et al, 2005), which is an adapted version from RAMS-5.04 (Pielke et al., 1992). The soil and vegetation model Leaf-3 is used to calculate the sensible and latent heat fluxes at the surface (Walko et al, 2000). CO_2 was not included in Leaf-3, therefore it was extended with the Farquhar model with the Ball-Berry equation (Farquhar et al., 1980, Collatz et al., 1991) to calculate photosynthesis rate. The configuration is the following :

- Two-way nesting was applied with grids resolution of 2 and 8 km.
- The land use is a simplified adaptation of the ECOCLIMAP database where classes have been aggregated into the 21 land use classes defined in Leaf.
- The Mellor-Yamada turbulence scheme is used.
- CO_2 sea fluxes are parameterized according to Takahashi et al. (1997).

This model will be referred to hereafter as RAMS-AMVU.

2.3 The RAMS version from the CEAM team

The CEAM team ran the RAMS (hereafter RAMS-CEAM) to simulate meteorology and the surface energy without including any CO_2 processes. The aim is to use in the future these meteorological results to simulate the transport of CO_2, fixing the fluxes by means of experimental data, similarly to Pérez-Landa et al. (2007).

Main characteristics of the RAMS-CEAM configuration:

- RAMS was run on four two-way nested domains at decreasing grid lengths of 36, 18, 6 and 2 km.
- The land use is a simplified adaptation of the ECOCLIMAP database where classes have been aggregated according to the Vrije University scheme.
- The LEAF-2 soil-vegetation surface scheme (Walko et al., 2000) was used to calculate sensible and latent heat fluxes exchanged with the atmosphere.

2.4 The RAMS version from the ALTERRA team

Hereafter, the results are denoted RAMS-ALTE. The ALTERRA team uses the RAMS model for which the main characteristics are :

- A two nested grid configuration is used at 6 km and 2 km resolution.
- The surface fluxes are simulated with the SWAPS-C surface scheme. There are four tiles per grid box: 1 water+3 most dominant land cover classes according to ECOCLIMAP. All classes are reclassified to either forest, grassland, urban; The SWAPS-C model parameters have been calibrated for LeBray (forest) and Cabauw (grassland) sites.
- CO_2 initialization and lateral boundaries forcing fields come from the LMDZ global model.
- Anthropogenic emissions are from the University of Stuttgart data sets (at 10 km resolution) and are disaggregated to hourly fluxes from urban pixels only.
- Marine fluxes are parameterized after Takahashi et al. (1997).

2.5 The non-hydrostatic MESO-NH model

Hereafter, the results of this model are noted MNH-CNRM.

The CNRM-Météo-France team ran the meso-scale non-hydrostatic model Meso-NH. The surface scheme ISBA-Ags (Noilhan et al., 1989; Calvet et al., 1998) coupled on-line includes biospheric CO_2 surface fluxes (assimilation, respiration) as well as the anthropogenic emissions. The chosen configuration is:

- A two-way nesting at 2 and 10 km resolution.
- The CO_2 concentrations are initialized with a vertical profile homogeneously over the domain.
- The lateral boundaries conditions for the carbon dioxide impose a zero gradient.
- CO_2 sea fluxes are parameterized according to Takahashi et al. (1997).

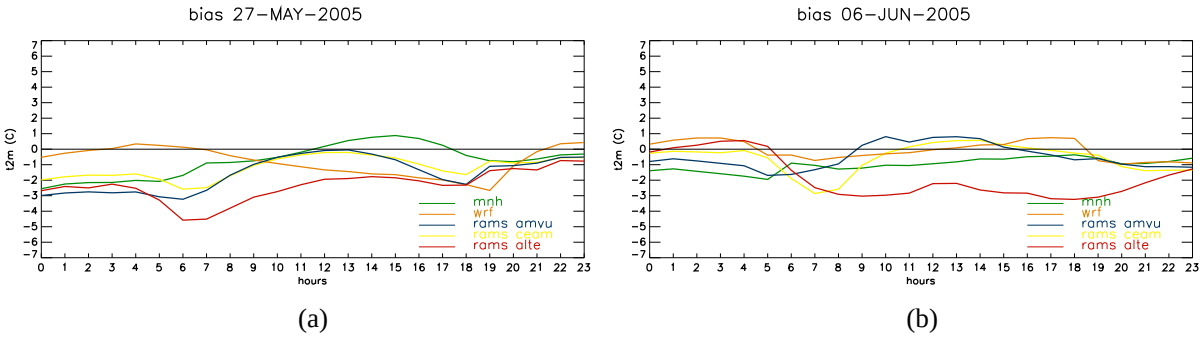

Fig. 2. Temporal evolution of the bias calculated for each model for the temperature at 2 m (T2M) on (**a**) 27 May and (**b**) 6 June.

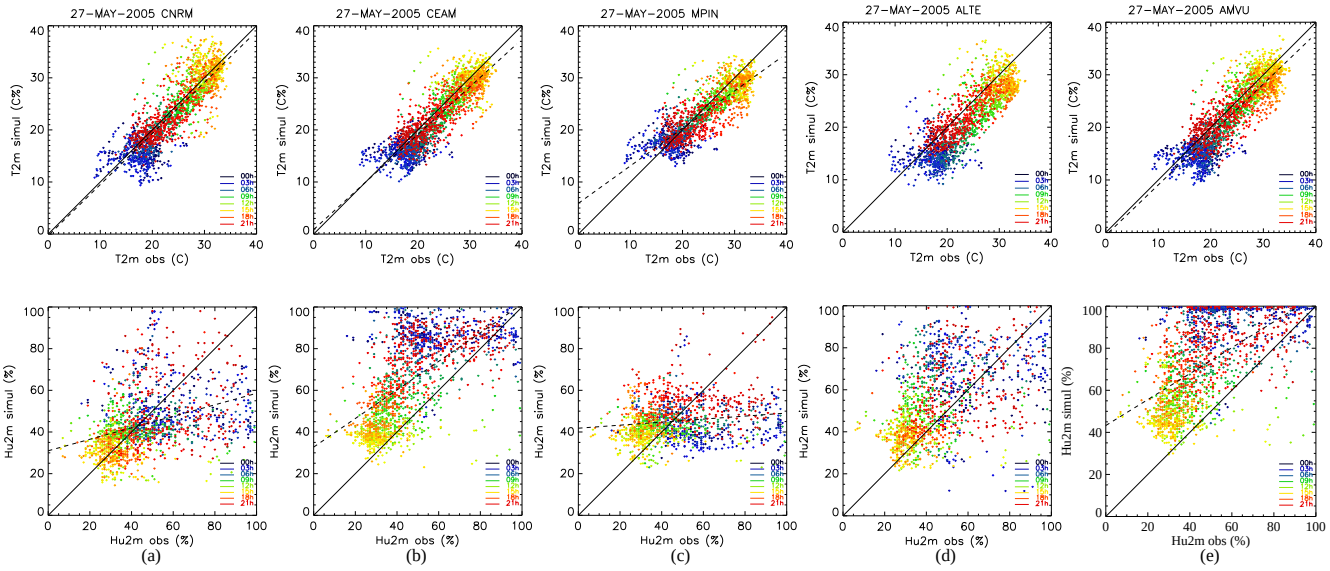

Fig. 3. Temperature at 2m and relative humidity at 2 m simulated vs observed for each model. Each point represents one hour for one station, i.e. 82 stations × 24 h on 27 May. (**a**) MNH-CNRM, (**b**)) RAMS-CEAM, (**c**) WRF-MPI, (**d**) RAMS-ALTE, (**e**) RAMS-AMVU.

3 Results

All the models have simulated the two cases of the CERES campaign. Comparisons between models and observations are given here for several variables:

- The temperature and relative humidity observed at the synoptic stations from the Météo-France network: 82 stations allow statistics and calculation of bias and rms for each model.
- The wind direction observed by the aircrafts.
- Surface fluxes of latent and sensible heat, CO_2 fluxes, net radiation at several sites (maize, wheat, pine forest).
- Radio-sounding made in LACS (Landes forest) at 23:00, 05:00, 08:00, 11:00, 15:00 and 17:00 UTC and at 11:00 UTC in TOUL (suburban station). The simulated vertical profiles of potential temperature between 0 and 3000 m are compared with observations.
- The CO_2 concentrations measured by the Piper Aztec and the Dimona aircrafts are compared to the model outputs along the aircrafts trajectories.

3.1 Meteorological variables

The temperature and the relative humidity at 2 m, respectively T2M and HU2M measured at 82 synoptic stations, included in the domain of simulation, are available from the French operational network. The comparisons with the simulations are made for hourly values.

The temporal evolution of the bias for T2m is shown in Fig. 2. There is no clear tendency of a daily cycle in the statistics of bias, although the T2M bias is negative for all models at 00:00 UTC on 27 May. This may be due to a

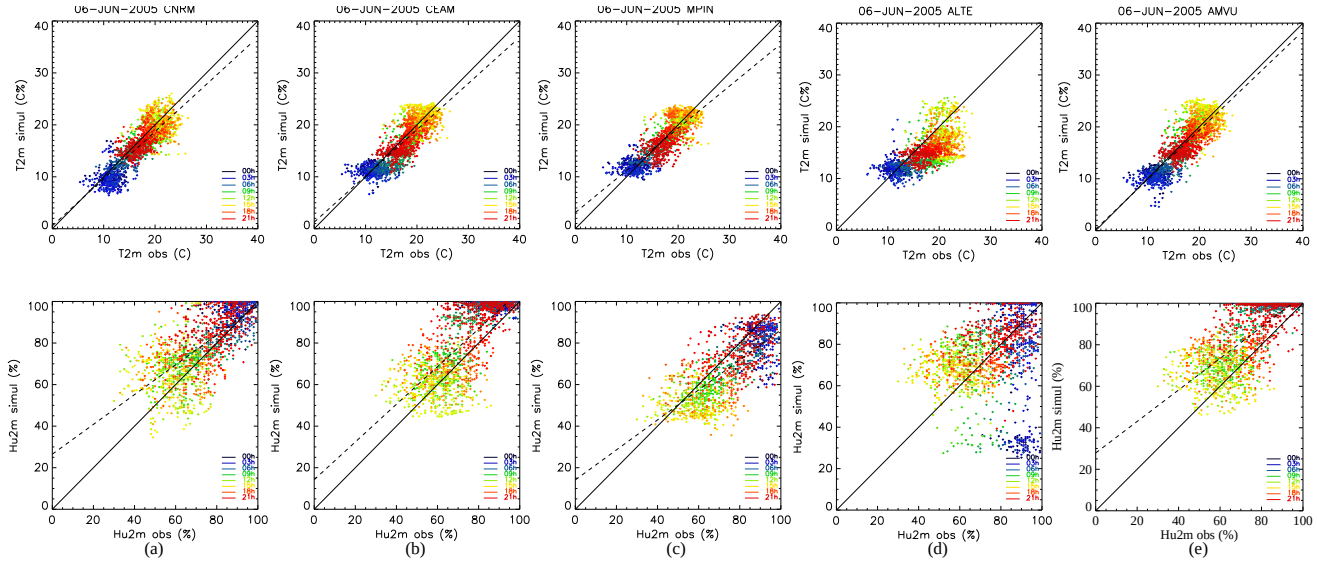

Fig. 4. Temperature at 2 m and relative humidity at 2 m simulated vs observed for each model. Each point represents one hour for one station, i.e. 82 stations × 24 h on 6 June. (**a**) MNH-CNRM, (**b**) RAMS-CEAM, (**c**) WRF-MPI, (**d**) RAMS-ALTE, (**e**) RAMS-AMVU.

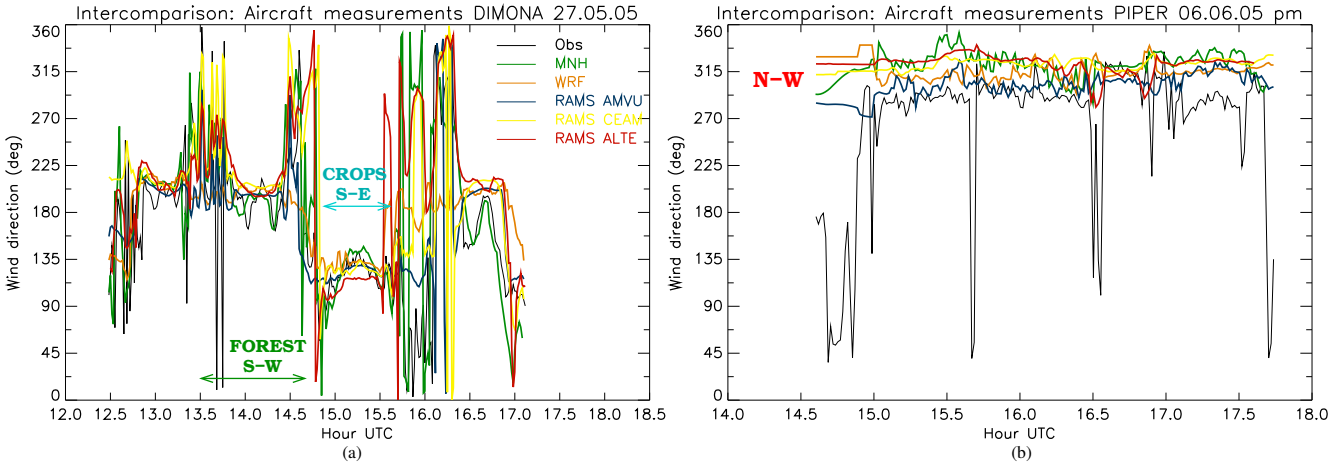

Fig. 5. Wind direction comparisons between the simulations and the observations: (**a**) from the Dimona aircraft on 27 May; (**b**) from the Piper-Aztec on 6 June.

problem in the initialization of the soil temperature. On 6 June, the bias is largely reduced during the night and remains low all day long except for the ALTE version of RAMS.

Figures 3 and 4 represent the T2M and HU2M simulated values against the observed ones, respectively for 27 May and 6 June, for all models.

It is clear, that the inter-model variability is larger for HU2M than for T2M during the two days. Moreover, the scatter for humidity is higher for nighttime than for daytime.

On 6 June, the scatter for temperature and humidity is less pronounced than on 27 May because of a stronger wind that limits the daily variations of temperature and humidity. In general, the statistical score are better for all model on 6 June than on 27 May, as shown in Table 4.

3.2 Characterization of the wind direction

At the regional scale, local atmospheric and surface conditions have a strong impact on the atmospheric dynamics. The CO_2 concentration distribution can be largely influenced by regional circulation as sea breeze for example. In fact, this situation is observed on 27 May. During this warm day, the sea breeze is developing along the coast and has been observed by the Dimona flight. Although, the synoptic situation generates a S-E wind over the cropland, the wind is from

Table 2. Comparisons between the measured volumetric soil moisture (WG, $m^3\,m^{-3}$) and the ECMWF analysis. Note that no precipitation occurred since the soil water measurement in MARM (18 May) and the day 27 May of the simulation.

	WG_{MARM} on 19 May $m^3.m^{-3}$	WG_{LACS} on 18 May $m^3.m^{-3}$	WG_{AURA} on 27 May $m^3.m^{-3}$
OBS	0.31	0.12	0.25
ECMWF on 27 May	0.25	0.13	0.27

Table 3. Summary of the models configurations.

	Domains resolutions	CO_2 initialization	CO_2 lateral boudaries conditions	Land cover	Surface Scheme
WRF-MPI	2 and 6 km	LMDZ fields	LMDZ fields	USGS 24 classes	offline VPRM model for CO_2
RAMS-AMVU	2 and 8 km	Homogeneous init	0 gradient	Ecoclimap 20 classes	Leaf-3+Farquhar model
RAMS-CEAM	2, 6, 18, 36 km	–	–	Ecoclimap 20 classes	Leaf-2
RAMS-ALTE	2 and 6 km	LMDZ fields	LMDZ fields	Ecoclimap 20 classes	SWAP-C
MNH-CNRM	2 and 10 km	Homogeneous init	0 gradient	Ecoclimap 62 classes	ISBA-A-gs

N-W over the forest and along the Atlantic Ocean coast, due to the sea breeze development. The comparison between the meso-scale models and the Dimona observations (Fig. 5a) shows that all the models are able to reproduce the sea breeze development.

On 6 June (Fig. 5b), all the models are in good agreement with the observed N-W wind from the Piper-Aztec data, allowing a Lagrangian Experiment Strategy during this day (see Sect. 3.5 for more details).

3.3 Surface fluxes

Different observed surface fluxes are compared to the simulated fluxes: net radiation (RN), sensible and latent heat (respectively H and LE) as well as the CO_2 flux. Only the RAMS-CEAM model does not simulate the surface flux of carbon dioxide.

Each model has its own CO_2 assimilation scheme (Farquhar type or A-gs type, on-line coupled with the atmosphere or using a diagnostic biosphere such as VPRM in WRF-MPI for example).

Thus, the response of the CO_2 surface flux to the atmospheric forcing presents a variability from one model to the other.

Figure 6 represents the 2D maps of CO_2 fluxes on 6 June at 10:00 UTC for each model. The oceanic fluxes are all from the Takahashi et al. (1997) parametrization (except WRF-MPI with zero oceanic fluxes) and are of the same order of magnitude. The other areas have quite different fluxes from one model to the other, especially with a positive signal in the North-Eastern part of the domain of the RAMS-ALTE model while the other ones simulate a net sink. This has to do with simulated clouds in the RAMS-ALTE that persist till about 10:30 UTC (compare Fig. 7c): these cause too low incident radiation levels with consequently low surface fluxes. The other models present also higher negative fluxes (larger uptake) above the cropland than above Les Landes forest, in agreement with the observation of the temporal series shown in Fig. 7. This figure compares the energy budget fluxes and the CO_2 fluxes at several sites: a winter crop, AURA (a), a pine forest, LEBR (b) and a summer crop MARM, (c), on 6 June.

For all models, the simulated surface fluxes compare very well to the observed ones at the winter crops stations (AURA), whereas the comparisons are less favourable at the summer crops stations especially on 27 May when the temperature is high and the fraction of vegetation is low due to a small development of the summer crops at this period (not shown here).

Nevertheless, on 6 June, at the AURA site, the sky is clear, all models are able to simulate RN and H and $SFCO_2$, LE is overestimated by most of the models.

On the other hand, the sky is cloudy in the western part of the domain. The net radiation decreases over the forest, in LEBR. Some models are not able to reproduce the clouds over this station and the net radiation is sometimes overestimated. At the LEBR site, all models are able to simulate the energy fluxes, although the latent heat is somewhat overestimated. For the summer crop site MARM, the latent heat flux is overestimated, while the sensible heat flux is overestimated by MNH-CNRM and RAMS-CEAM. One can note that the observed energy fluxes are not in balance in MARM, maybe

Table 4. Mean temperature at 2 m (T2M) and relative humdity at 2 m (HU2M) RMS and Bias on 27 May and 6 June.

	WRF-MPI	RAMS-AMVU	RAMS-CEAM	RAMS-ALTE	MNH-CNRM
RMS T2M 27 May	3.2	3.8	3.1	4.9	3.4
RMS T2M 6 June	2.2	3.1	2.3	3.2	2.5
RMS HU2M 27 May	19.8	22.9	23.7	19.8	19.8
RMS HU2M 6 June	12.2	11.8	13.0	17.8	12.2
Bias T2M 27 May	−0.8	0.4	−1.2	−3.4	−0.8
Bias T2M 6 June	−0.1	0.3	−0.6	−1.8	−0.9
Bias HU2M 27 May	2.2	11.7	17.7	8.3	−3.0
Bias HU2M 6 June	−6.6	1.6	7.3	−2.7	5.5

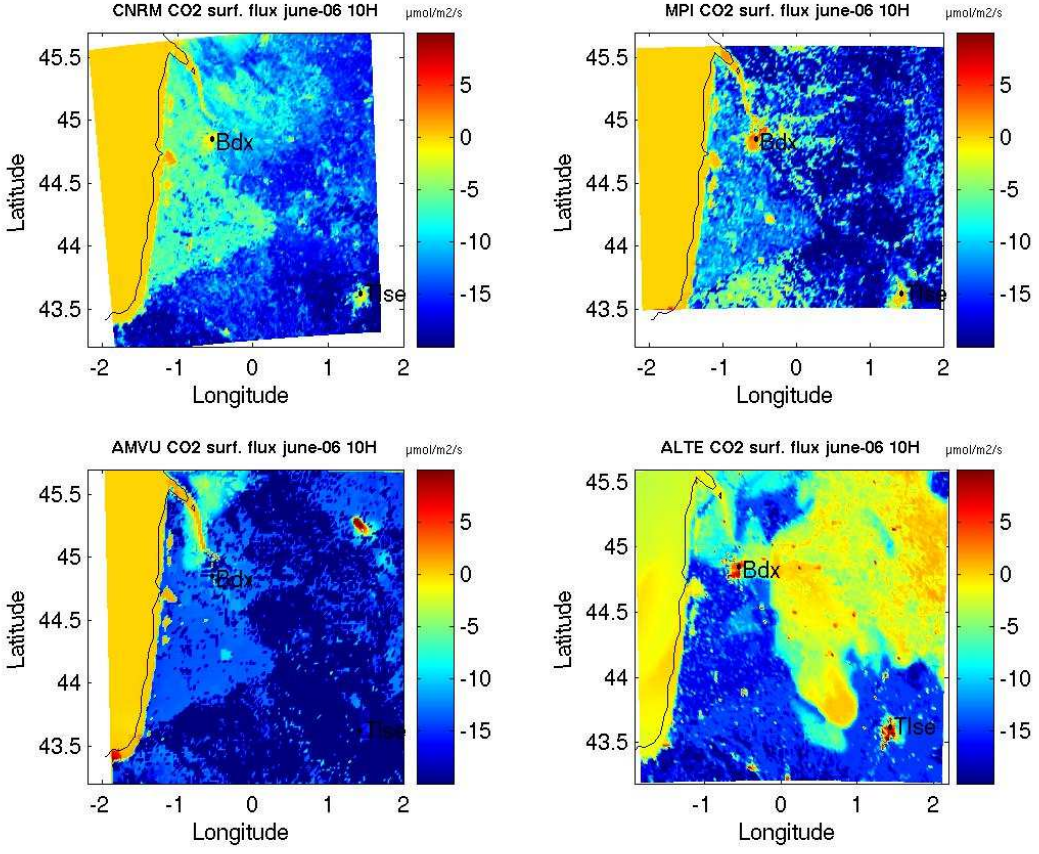

Fig. 6. CO_2 surface fluxes at 10:00 UTC on 6 June by the different models.

due to an underestimation of the observed latent heat flux.

In general, all the models simulate relatively well the surface flux of CO_2, particularly at the crop sites, AURA and MARM. Generally, the surface fluxes are simulated better on 6 June than on 27 May, mainly due to a lower LAI and a higher fraction of bare soil on 27 May. Nevertheless, the latent heat flux is often overestimated by most of the models.

3.4 Boundary Layer development

During IOP days, radiosounding (RS) balloons were launched in les Landes forest, at LACS every 3 h. In addition, a radiosounding was launched in Toulouse (TOUL) at 11:00 UTC every IOP days.

The observed and simulated vertical profiles of potential temperature are compared in Fig. 8.

On 27 May, all models underestimate the ABL height, particularly in the TOUL site. Nevertheless, at 11:00 UTC, in TOUL (Fig. 8b), all the models are able to simulate a lower

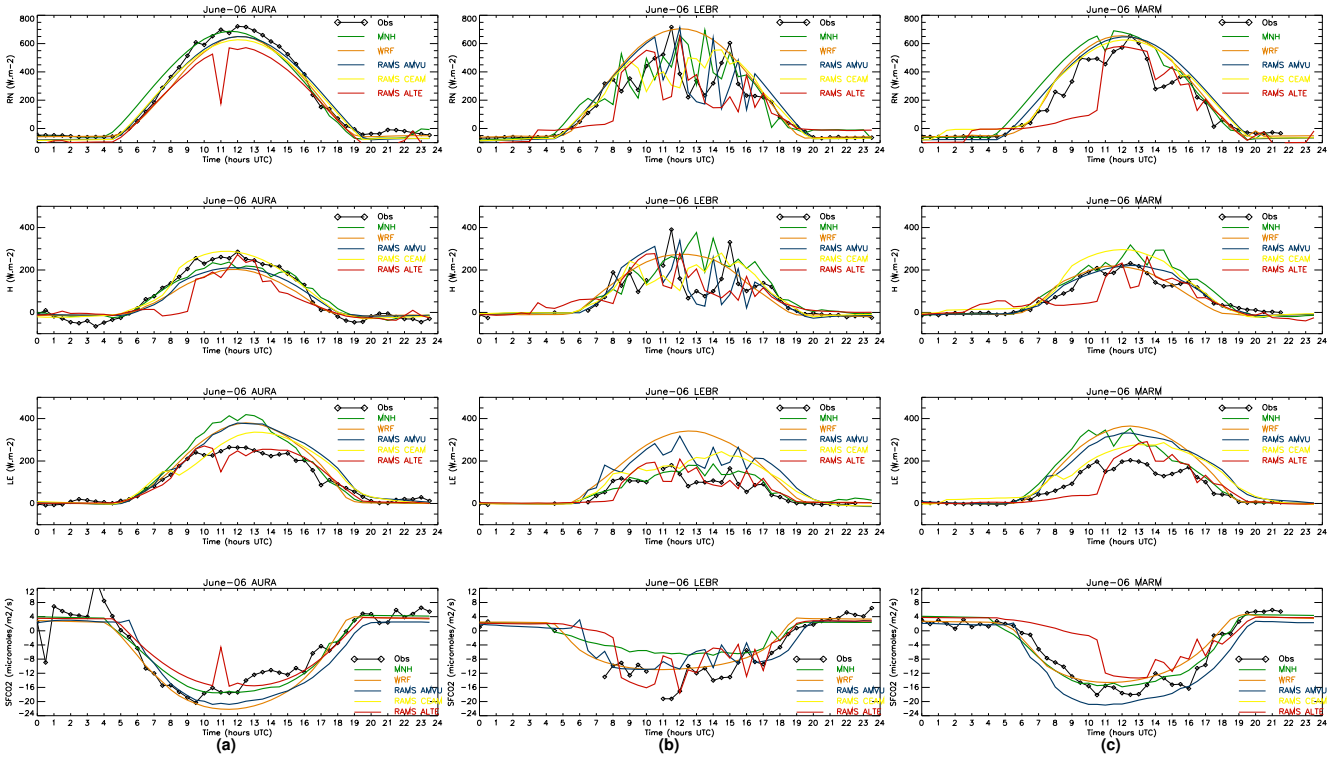

Fig. 7. Time series of surface fluxes, RN, H, LE and CO_2 on 6 June: (**a**) AURA (wheat); (**b**) LEBR (pine forest); (**c**) MARM (maize).

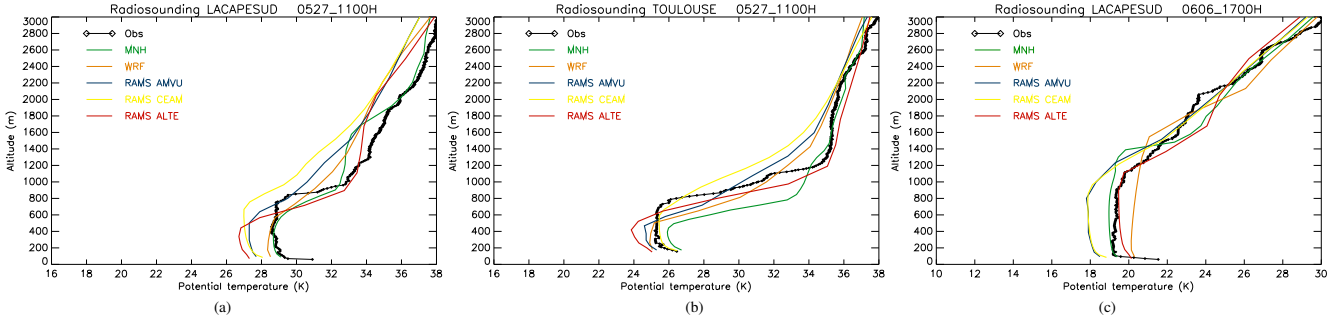

Fig. 8. Vertical profiles of potential temperature observed by radio-soundings and simulated on 27 May at 11:00 UTC (**a**) in LACS (forested site); (**b**) in TOUL (eastern); (**c**) on 6 June at 17:00 UTC.

boundary layer height than in LACS (Fig. 8a) as shown in the observations.

On 6 June, the ABL height is very well simulated by RAMS-ALTE. Two models (RAMS-CEAM and RAMS-AMVU) underestimate the potential temperature, whereas two others (MNH-CNRM and WRF-MPI) overestimate the boundary layer height.

The ABL height is a key variable in modeling atmospheric CO_2 since surface fluxes are to first order mixed up to this altitude, causing the atmospheric CO_2 concentration to be underestimated when the ABL is overestimated, and vice versa, assuming a surface source; with a sink this behavior reverses (Gerbig et al., 2007). The comparisons between the RS and the simulations reveal discrepancies between models and errors on the evaluation of the ABL height despite the agreement between modeled and observed sensible heat fluxes (see Sect. 3.3).

This suggests that some key elementary processes in boundary layer development, as entrainment at the top, may not be well captured by some of the models.

3.5 Atmospheric CO_2 simulation

All models simulate the CO_2 concentrations as a function of the surface fluxes (anthropogenic and biogenic) and the boundary layer dynamics, except the CEAM version of RAMS.

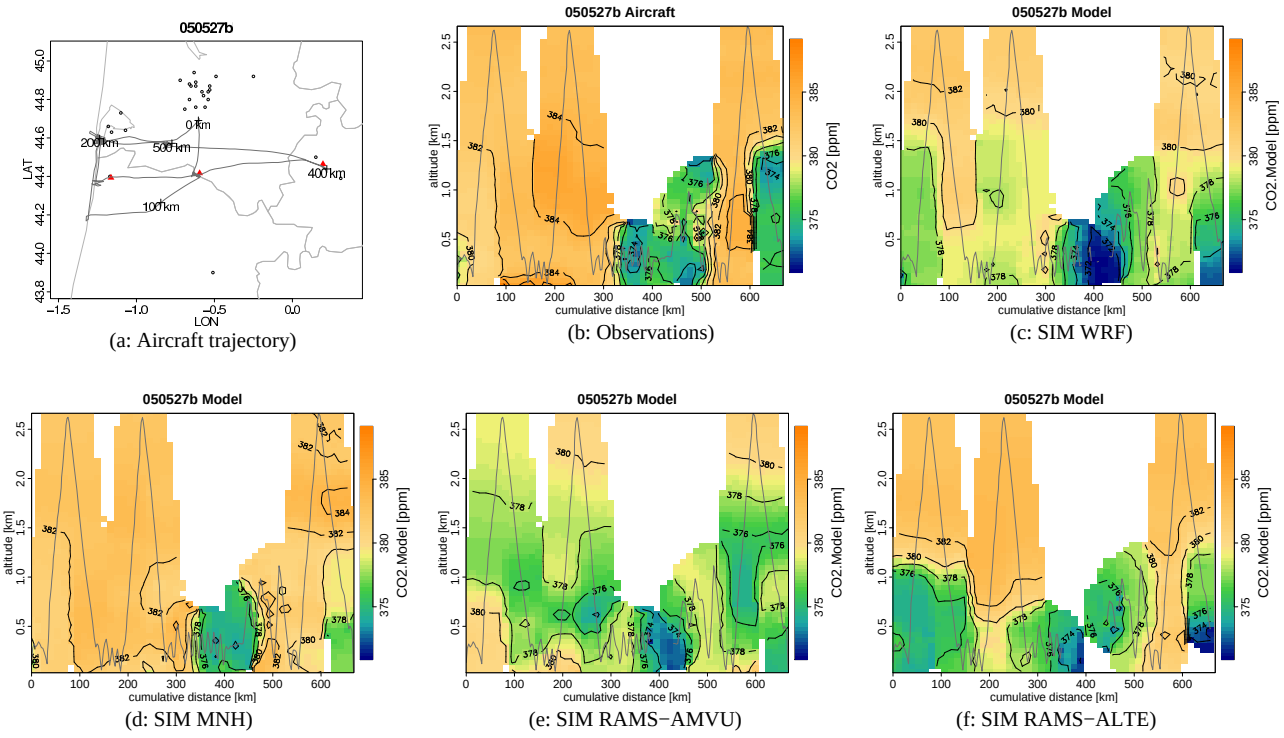

Fig. 9. CO_2 concentrations observed and simulated along the aircraft trajectory represented on (**a**); the observations are displayed on (**b**), (**c**), (**d**), (**e**) and (**f**) are the respective simulations of WRF-MPI, MNH-CNRM, RAMS-AMVU and RAMS-ALTE.

During the CERES campaign, the CO_2 concentrations have been measured by aircrafts, above Les Landes forest, the Atlantic Ocean coast or above the agricultural areas. On 27 May, as shown in Fig. 9a, the Dimona aircraft flew over the forest and over the cropland. The aircraft was equipped with instruments to measure trace gases including CO_2, CO, NO, NO_2, NOy, O_3 and aerosols, as well as standard meteorological and navigational parameters (Dolman et al., 2006). CO_2 in-situ data from a modified closed path Licor 6262 (Schmitgen et al., 2004) and an open-path Licor 7500 have been combined and adjusted to match the measurements of simultaneously collected flask samples; this is necessary since the continuous instrument is only calibrated on ground before and after, but not during each flight, and thus is not used as independent measurement. The combined record of high frequency but less precise open path, slower but more precise close path and accurate flask measurements give a 10 Hz response time series at an accuracy of 0.5 ppmv. Many vertical profiles have been performed during this flight (see altitude of flight in Fig. 9b). The CO_2 in-situ observations, in Fig. 9b show a strong gradient up to 15 ppmv between the cropland and the forest. This gradient is due to a combination of a strong assimilation by the winter crop and a recirculation of nocturnal respired CO_2 in the sea-land breeze pattern (Sarrat et al., 2007; Ahmadov et al., 2007). All the models are able to reproduce this gradient and especially the low concentrations measured over the eastern part of the flight related to a high assimilation of CO_2 over the agricultural area.

During the same day, the Piper Aztec aircraft measured the CO_2 by infrared absorption (CONDOR system), making vertical profiles above the forest and the cropland, in the morning and the afternoon. These vertical profile provide information on the ABL height and the CO_2 concentrations in and above the ABL. Figure 10 shows the height of the ABL as a function of the mean CO_2 concentration in the ABL, at both sites. It shows that the observed mean CO_2 concentrations decrease in the ABL when the ABL height increases. This decrease is related to CO_2 vertical mixing in the layer but also to photosynthesis activity which depletes the ABL, off set by entrainment at the top of the ABL. The decrease is also more visible at the MARM site (cropland) than at the LACS site (forest) although the ABL height is smaller. All the models are able to reproduce this general trend.

On 6 June a North-West regular wind prevailed and allowed a “Lagrangian Experiment”, based on in-situ aircraft measurements. This experiment deals with the in-flow air sampling in the morning (near the oceanic coast line) and the sampling of the same air mass downstream the forest a few hours latter, depending on the wind speed and the air mass displacement, as shown in Fig. 11.

The time series of CO_2 concentrations measured by the Piper-Aztec aircraft are compared to the simulations along the aircraft trajectory. The observed concentrations in the

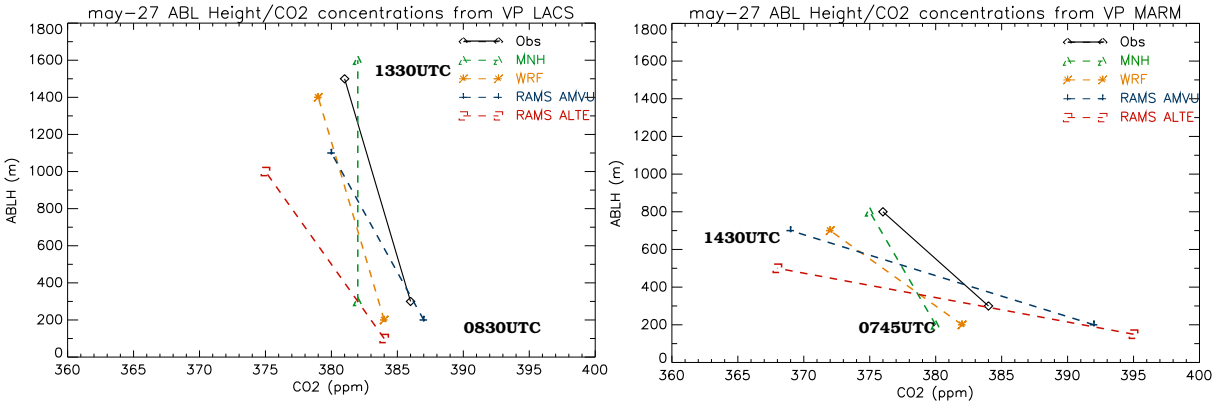

Fig. 10. ABL height as a function of CO_2 concentrations in the ABL at LACS (left panel) and MARM (right panel) sites.

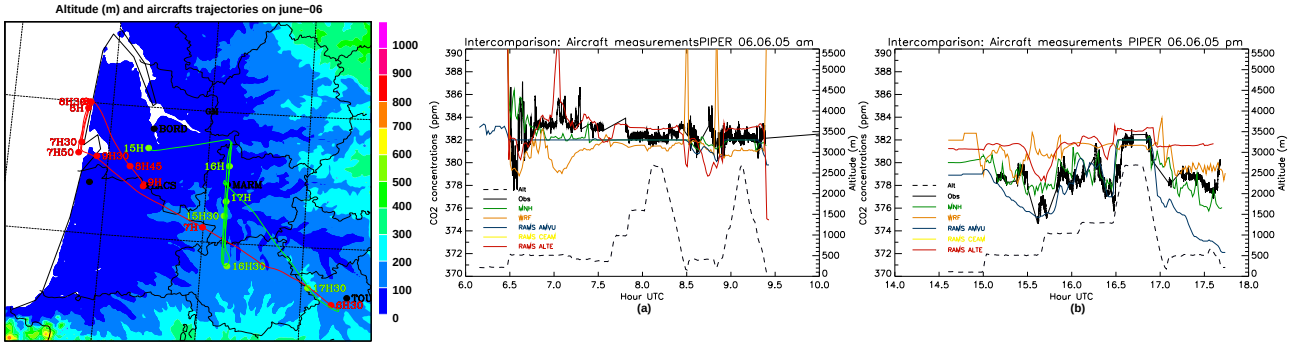

Fig. 11. Surface altitude of the domain with aircraft trajectories: red=morning flight and green=afternoon flight. Times series of CO_2 concentrations observed by the Piper-Aztec aircraft and simulated in the morning (**a**) and in the afternoon (**b**). The dashed lines represent the altitude (asl) of flight.

morning (Fig. 11a) are almost constant and regular during the flight, between 382 and 383 $\pm$1 or 2 ppmv, depending of the altitude. The simulations give also constant concentrations except for WRF-MPI that occasionally overestimates the CO_2 at low altitude. In the afternoon flight, (Fig. 11b), downstream the forest, the observed concentrations are lower, except above the ABL, principally due to net assimilation of carbon dioxide by the ecosystem. The WRF-MPI and RAMS-ALTE models tend to overestimate the afternoon concentrations, despite good CO_2 surface fluxes shown in Sect. 3.3. RAMS-AMVU underestimates the concentrations when the aircraft is at low altitude, in relation with its tendency to overestimate the assimilation fluxes (Sect. 3.3). RAMS-AMVU also exaggerates the vertical extent of CO_2 depletion. This depletion above 1 km originates above mountain ranges outside the CERES domain and is then advected into the domain (not shown here). It has been discovered lately that this is caused by an error in the mass balance in RAMS above slopes. A publication about this is intended.

However, the simulations are in reasonable agreement with the observations, showing the air mass depleting with CO_2 while it moves across the forest.

In general, the regional models are able to simulate with reasonable accuracy the larger scale atmospheric CO_2 concentrations, despite some remaining discrepancy at smaller spatial and temporal scale.

4 Conclusions

Two contrasting golden days of the CERES campaign are selected and simulated by 5 meteorological meso-scale models. A protocol of simulation is applied in order to run as much as possible within a common framework:

– A similar inner domain of simulation at 2 km resolution is used.

– Meteorological variables are initialized and forced at the lateral boundaries by the ECMWF model as well as the surface initialization.

– the ECOCLIMAP land cover serves as the main land cover map.

For these two days some comparisons between the models and the observations are performed in order to evaluate the

outputs of the meso-scale modeling. These comparisons include:

- The meteorological variables: temperature and relative humidity at 2m. The hourly data are provided by 82 meteorological stations data allowing rms and bias calculation for each models.
- The surface fluxes of net radiation, sensible and latent heat fluxes, CO_2 surface flux, measured by eddy correlations at several sites.
- The potential temperature in the boundary layer measured during radio-soundings in the forested central site.
- The CO_2 concentrations observed during the aircrafts flights above the Atlantic coast, the forest and the cropland.

All these comparisons show the ability of meteorological meso-scale models to represent the atmospheric carbon dioxide distribution satisfactory, in general agreement with the observations. The complex spatial distribution as well as the temporal evolution of CO_2 in interaction with the surface fluxes are realistically simulated compared to the aircrafts observations. This raises hope that the mesoscale models may provide adequate transport of CO_2 and other tracers at high resolution.

The dynamic parameters at the synoptic scale (temperature and relative humidity at 2 m) but also at the local scale (potential temperature at various sites) are previously validated in confrontation with the respective observations. All the models are able to simulate the surface meteorology reasonably well. Nevertheless, some discrepancies are pointed out in this study: a common cold bias in the initial temperature at 2 m appears in this intercomparison. This may be due to an initialization problem, that has to be checked and improved. Also, the boundary layer height modeling, as a key process in meso-scale modeling, still causes some discrepancy. Particularly, the entrainment at the top of the boundary layer has to be checked as a key process in CO_2 modeling (Vilá-Guerau et al., 2004). The latent heat flux is often overestimated by most of the models.

The quantification of continental sources and sinks of CO_2 will be improved by regional inversion. But the validated regional modeling in forward mode is a prior to this top-down approach. Even for the bottom-up models, the uncertainties remain high, compared to what would be required for really accurate inversion calculations. The critical points listed above are related to each other and must be examined in order to improve the atmospheric CO_2 modeling at the regional scale. In fact, with the present set up, it is difficult to distinguish between differences caused by (1) determination of the surface fluxes of CO_2; (2) determination of the atmospheric transport of CO_2. A numerical experiment imposing common surface fluxes to all models could be usefull for the interpretation of the results, for the future.

Acknowledgements. The authors would like to thank all the colleagues and CarboEurope partners who have contributed to the CERES campaign. Particularly, we address our acknowledgements to the CESBIO, Alterra and INRA teams who provided the surface fluxes observations, the 4M- Météo France team for the radio soundings, the aircaft teams of SAFIRE – Météo France for the Piper-Aztec and LSCE for the CONDOR instrument and B. Neininger from Metair for the Dimona.

Edited by: T. Laurila

References

Ahmadov, R., Gerbig, C., Kretschmer, R., Koerner, S., Neininger, B., Dolman, A., and Sarrat, C.: Mesoscale covariance of transport and CO_2 fluxes: evidence from observations and simulations using the WRF-VPRM coupled atmosphere-biosphere model, J. Geophys. Res., in press, 2007.

Bousquet, P., Ciais, P., Monfray, P., Balkanski, Y., Ramonet, M., and Tans, P.: Influence of two atmospheric transport models on inferring sources and sinks of atmospheric CO_2, Tellus, 48B, 568–582, 1998.

Calvet, J.-C., Noilhan, J., Roujean, J.-L., Bessemoulin, P., Cabelguenne, M., Olioso, A., and Wigneron, J.-P.: An interactive vegetation SVAT model tested against data from six contrasting sites, Agri. For. Meteor., 92, 73–95, 1998.

Champeaux, J., Fortin, H., and Han, K.-S.: Spatio-temporal characterization of biomes over south-west of France using SPOT/VEGETATION and Corine Land Cover datasets, IGARSS'05 Proceedings, 2005.

Dolman, A., Noilhan, J., Durand, P., Sarrat, C., Brut, A., Butet, A., Jarosz, N., Brunet, Y., Loustau, D., Lamaud, E., Tolk, L., Ronda, R., Miglietta, F., Gioli, B., Magliulo, E., Esposito, M., Gerbig, C., Koerner, S., Galdemard, P., Ramonet, M., Ciais, P., Neininger, B., Hutjes, R., Elbers, J., Warnecke, T., Landa, G., Sanz, M., Scholz, Y., and Facon, G.: CERES, the Carboeurope Regional Experiment Strategy in: les Landes, South West France, May–June 2005, BAMS, 87, 1367–1379, 2006.

Freitas, S. R., Longo, K. M., Silva Dias, M. A. F., Silva Dias, P. L., Chatfield, R., Prins, E., Artaxo, P., Grell, G. A., and Recuero, F.S.: Monitoring the transport of biomass burning emissions in South America, Environ. Fluid Mech., 5, 135–167, 2005.

Gerbig, C., Lin, J., Wofsy, S., Daube, B., Andrews, A., Stephens, B., Bakwin, P., and Grainger, A.: Toward contraining regional scale fluxes of CO_2 with atmospheric observations over a continent: 1. Observed spatial variability from airborne platforms, J. Geophys. Res., 108(D24), 4756, doi:10.1029/2002JD003018, 2003.

Gerbig, C., Koerner, S., and Lin, J. C.: Vertical mixing in atmospheric tracer transport models: error characterization and propagation, Atmos. Chem. Phys. Discuss., 7, 13 121–13 150, 2007.

Lauvaux, T., Uliasz, M., Sarrat, C., Chevallier, F., Bousquet, P., Lac, C., Davis, K. J., Ciais, P., Denning, A. S., and Rayner, P.: Mesoscale inversion: first results from the CERES campaign with synthetic data, Atmos. Chem. Phys. Discuss., 7, 10 439–10 465, 2007.

Noilhan, J. and Planton, S.: A simple parametrization of land surface processes for meteorological models, Mon. Weather Rev., 117, 536–549, 1989.

Pathmathevan, M., Wofsy, S., Matross, D., Xiao, X., Dunn, A., Lin, J., Gerbig, C., Munger, J., Chow, V., and Gottlieb, E.: A Satellite-based biosphere parameterization for Net Ecosystem CO_2 Exchange: Vegetation Photosynthesis and Respiration Model (VPRM), Global Biogeochem. Cy., doi:10.1029/2006GB002735, in press, 2007.

Pérez-Landa, G., Ciais, P., Gangoilti, G., Palau, J., Carrara, A., Gioli, B., Miglietta, F., Schumacher, M., Millan, M., and Sanz, J.: Mesoscale circulations over complex terrain in the Valencia coastal region, Spaign – Part 2: Modeling CO_2 transport using idealized surface fluxes, Atmos. Chem. Phys., 7, 1851–1868, 2007,
http://www.atmos-chem-phys.net/7/1851/2007/.

Pielke, R. A., Cotton, W. R., Walko, R. L., Tremback, C. J., Lyons, W. A., Grasso, L. D., Nicholls, M. E., Moran, M. D., Lee, D. A. W. T. J., and Copeland, J. H.: A Comprehensive Meteorological Modeling System – Rams, Meteorol. Atmos. Phys., 49, 69–91, 1992.

Rödenbeck, C., Houweling, S., Gloor, M., and Heimann, M.: CO_2 flux history 1982–2001 inferred from atmospheric data using a global inversion of atmospheric transport, Atmos. Chem. Phys., 3, 1919–1964, 2003,
http://www.atmos-chem-phys.net/3/1919/2003/.

Sarrat, C., Noilhan, J., Lacarrère, P., Donier, S., Lac, C., Calvet, J.-C., Dolman, A., Gerbig, C., Neininger, B., Ciais, P., Paris, J., Boumard, F., Ramonet, M., and Butet, A.: Atmospheric CO_2 modeling at the regional scale in : Application to the CarboEurope Regional Experiment, J. Geophys. Res., 112, D12105, doi:10.1029/2006JD008107, 2007.

Schmitgen, S., Geiß, H., Ciais, P., Neininger, B., Brunet, Y., Reichstein, M., Kley, D., and Volz-Thomas, A.: Carbon dioxide uptake of a forested region in southwest France derived from airborne CO_2 and CO measurements in a quasi-Lagrangian experiment, J. Geophys. Res., 109, D14302, doi:10.1029/2003JD004335, 2004.

Skamarock, W., Klemp, J., Dudhia, J., Gil, D., Barker, D., Wang, W., and Powers, J.: A description of the advanced research WRF (Version 2), NCAR Technical Note, 2005.

Takahashi, T., Feely, R.,Weiss, R., Wanninkhof, R., Chipman, D., Sutherland, S., and Takahashi, T.: Global air-sea flux of CO_2 : An estimate based on measurements of sea-air pCO_2 difference, Proc. Natl. Acad., 94, 8292–8299, 1997.

Tans, P., Fung, I., and Takahashi, T.: Observational constraints on the global atmospheric CO_2 budget, Science, 247, 1437–1438, 1990.

Vilá-Guerau de Arellano, J., Gioli, B., Miglietta, F., Jonker, H., Baltink, H., Hutjes, R., and Holtslag, A.: Entrainment process of carbon dioxide in the atmospheric boundary layer, J. Geophys. Res., 109, D18110, doi:10.1029/2004JD004725, 2004.

Walko, R. L., Band, L. E., Baron, J., Kittel, T. G. F., Lammers, R., Lee, T. J., Ojima, D., Pielke, R. A., Taylor, C., Tague, C., Tremback, C. J., and Vidale, P. L.: Coupled atmosphere-biophysics-hydrology models for environmental modeling, J. Appl. Meteorol., 39, 931–944, 2000.